

CHAPTER 4

Specificity in Photocatalysis

YARON PAZ*^a^aDepartment of Chemical Engineering, Technion, Haifa 32000, Israel

*E-mail: paz@tx.technion.ac.il

4.1 Introduction

Free radicals play dominant roles in almost all photocatalytic processes. Among these free radicals, the most prominent are the hydroxyl radicals, formed primarily from oxidation of water or OH⁻ by photogenerated holes. Superoxide anion radicals, formed by reduction of di-oxygen by photogenerated electrons, are no less important. Their formation reduces the recombination rate.¹ In addition, superoxides participate in the process as active species (usually in the secondary steps of degradation) and, upon reacting with protons, as a secondary source for OH radicals *via* homolytic cleavage of H₂O₂. Other radicals, of lesser importance in photocatalysis, are oxygen atoms. The large differences between the redox potential of the hydroxyl radical and that of many organic compounds, together with very low activation energy and weak steric hindrance (typical for small size radicals), are manifested by strong activity that does not differentiate between different organic compounds.

The lack of sensitivity to the type of contaminants is usually regarded as one of the strengths of photocatalysis, as it means that there is no need to pre-design the photocatalyst for each, specific contaminant. In that manner, a single photocatalyst may handle a stream containing a mixture of contaminants, with minimal need for on-line characterization of the feed.

RSC Energy and Environment Series No. 14

Photocatalysis: Fundamentals and Perspectives

Edited by Jenny Schneider, Detlef Bahnemann, Jinhua Ye, Gianluca Li Puma,
and Dionysios D. Dionysiou

© The Royal Society of Chemistry 2016

Published by the Royal Society of Chemistry, www.rsc.org

Nevertheless, the real situation is far more complex. Mixed streams may contain hazardous contaminants together with organic contaminants of low toxicity. In many cases, the toxic material is in low concentration, whereas the less toxic compounds are the majority. Obviously, in such cases, it is preferable to degrade the more toxic material, even at the expense of lower degradation rates for the less harmful components.

Many of the highly hazardous materials are non-biodegradable or even toxic for bacteria. A synergistic combination of several techniques, for example, photocatalysis and biological treatment^{2,3} or sonolysis + photocatalysis pretreatment may provide the right solution.⁴ Here, again, the inherent non-specificity of photocatalysis considerably limits the benefits of the combined advanced oxidation processes (AOP)-biological approach. The fact that the adsorption coefficient of many of the chlorinated xenobiotic compounds on oxides is very low due to their hydrophobic nature aggravates this problem. Hence, it is important to direct the AOP treatment towards the degradation of non-biodegradable compounds or towards compounds that might render the use of biological treatment techniques.

Photocatalysts that operate specifically, *i.e.* handle compounds in a pre-designed preferential manner, may provide the right solution for the above-mentioned situations. Specificity is of large added value also in all cases where toxic intermediates are formed and released, as in the gas-phase photocatalytic degradation of trichloroethylene (TCE), where phosgene and dichloroacetyl chloride might be released.⁵

The increased interest in green chemistry and in the possibility of using photocatalysis for the production of valuable compounds is closely related with developing means to control the end-products, *i.e.* to increase the selectivity away from mineralized products (CO₂, water, mineral ions) towards partially oxidized (or reduced) products, having large economic value. Such products can be utilized only if they are resistant to photocatalysis or, alternatively, can be easily separated from the product stream.

In what follows, this chapter discusses various ways to obtain preferential degradation (defined hereby as reactants' specificity) and selectivity (defined hereby as products' specificity). Despite growing awareness of the need for specificity in photocatalysis, the number of review articles on this issue is very low. Interested readers are directed to a former review.⁶ Notably, most of the research work compiled for this chapter did not originate from papers dedicated to specificity, but rather from those aimed at other aspects of photocatalysis, which occasionally presented data that is of relevance to this chapter. In that sense, one of the aims in writing this chapter is to increase awareness in the community of the need for better ways to obtain specificity, both on the reactants' side and on the products' side.

Within the context of this chapter, relative efficiency is defined as the ratio between the photocatalytic rates with modified substrates *versus* the photocatalytic rates measured under the same conditions and the same amount of non-modified photocatalyst. This definition suffers from being arbitrary to some extent since it does not declare whether the relevant rates are the

rates of disappearance of the target molecules or the rates of appearance of end-products. In cases where the reaction mechanism with modified substrates is the same as with non-modified the two alternatives are expected to yield similar values. However, this is not the case when modifying the photocatalyst alters the mechanism. Generally speaking, since specificity in photocatalysis is usually related to preferential degradation of highly toxic compounds, comparing the disappearance rates of the target molecules should be of more importance than comparing mineralization rates.

In the past, awareness of the importance of specificity was very low, as reflected in the low number of publications dedicated to specificity. Still, a lot of useful information can be obtained by analyzing publications that, as part of presenting new or modified photocatalysts, compared the degradation rates of various reactants. For most cases, these experiments were performed as sets of single-contaminant experiments. This raises a question mark regarding their relevance for solutions containing mixtures of contaminants. Generally speaking, relative rates that are measured in single-component experiments should be regarded as providing qualitative guidelines and should not be taken as predictive values for mixed stream situations, as indeed was found for a mixture containing oxalic acid, formic acid and formaldehyde.⁷ As a rule of thumb, the degradation rates of strongly adsorbed contaminants are not expected to vary by much in the presence of other contaminants, whereas the degradation rates of contaminants that adsorb weakly are expected to change significantly in the presence of other contaminants. Another parameter that affects the difference between mono- and multi-component measurements is the formation of intermediates (or end-products) that influence the degradation of cross contaminants. This was the situation in the degradation of 2-chlororophenol; the degradation rate of which was found to be affected by the presence of nitrate ions formed during the degradation of co-existing 2-nitrophenol.⁸

In writing this chapter the photocatalytic process is divided into its major steps and each step is analyzed from the point of view of inducing specificity. This structuring of the chapter is quite different from that of similar reviews. Nevertheless, such sub-division may assist researchers in developing new approaches for specificity. Notably, however, in many cases where specificity was observed the exact reason remained obscure.

4.2 Mass Transport to the Photocatalyst and Adsorption

The rationale that controlling adsorption may be used to obtain specificity is based on the pre-assumption that the degradation rates obey the Langmuir-Hinshelwood (LH) kinetics, which, for single-sites adsorption, is:

$$r \equiv -\frac{dC_A}{dt} = k_r g_A = k_r \frac{K_A C_A}{1 + \sum K_i C_i} \quad (4.1)$$

where C_i is the concentration of species i in the bulk, k_r is the reaction rate constant, and K_i is the equilibrium constant of adsorption for species i . Quite surprisingly, the measuring of kinetics having a concentration dependency similar to that of the LH expression does not necessarily imply that adsorption on the surface of the photocatalyst is a strict pre-requisite for photocatalysis.⁹ This is further supported by the observation of “remote degradation” phenomena.^{10–12} Nonetheless, mass-transport to the vicinity of the active sites, as well as adsorption, is of major importance in governing the rate of photocatalysis. Consequently, controlling mass transport and adsorption in a manner that prefers one compound over another became a major tool for achieving specificity. Indeed, competitive adsorption is often the key in photodegradation competition as observed by Zahraa *et al.* who studied the co-degradation of atrazine and salicylic acid.¹³

In what follows we discuss the ways by which the various characteristics of adsorption were utilized to obtain specificity. Cases in which specificity was non-intentionally documented are analyzed as well. Notably, however, in such cases there might be several co-existing explanations for the observed specificity phenomena. Moreover, many of the publications that reported on specificity phenomena were silent with respect to reasoning.

4.2.1 Complexation in the Fluid Phase

Complexation of specific reactants in a way that either increases their solubility in the solvent or alters their tendency to be adsorbed on the surface may serve to obtain specificity. An example for this approach was presented by Wang *et al.* who used chloride ions to complex Hg(II), thus retarding its photocatalytic reduction without affecting that of Cr(VI) that was co-presented in the solution. That way, the researchers were able to separate the two despite their similar redox potential (0.85 V for Hg^{2+}/Hg and 0.82 V for $\text{Cr}_2\text{O}_7^{2-}/\text{Cr}^{3+}$).¹⁴ Likewise, it was found that the presence of chlorides, sulfates and phosphates altered the relative oxidation rates of salicylic acid, aniline and ethanol.¹⁵ For example, the presence of 0.001 M Na_3PO_4 reduced the photodegradation rate of salicylic acid by 64% but reduced that of ethanol by no more than 44%. Generally speaking, this effect of the co-solutes on specificity was found to be too mild to consider it a practical approach. In addition, this change in the relative rates was accompanied with a decrease in the oxidation rates for all studied compounds.

When it comes to the liquid phase, adsorption reflects a delicate balance of interactions between adsorbate–adsorbent, solvent–adsorbate and solvent–adsorbent. Altering the solvent should have an effect on the tendency for adsorption. Each solvent has its specific interaction with a specific solute, therefore it can be expected that the relative adsorbabilities (and, consequently, the relative degradation rates) will be affected upon changing the solvent. Indeed, it was shown that the ratio of alcohol to ketone adsorption on TiO_2 could vary by a factor as large as 22 by using appropriate solvents.¹⁶

Notably, however, making use of this ability to control relative adsorption to obtain specificity is quite difficult, since almost all organic solvents tend to degrade photocatalytically.

A correlation between the dielectric constant of the solvent and the selectivity was found also in the photocatalytic reduction of CO_2 by TiO_2 nanocrystals embedded in SiO_2 .¹⁷ Here, the carbon dioxide was reduced in the presence of nitrate ions, yielding a mixture of carbon monoxide, formate ions, ammonia and urea. The higher the dielectric constant was, the more urea and ammonia were obtained at the expense of formate and CO. The results were explained by the effect of the dielectric constant of the solvents on the dissociation of the nitrate salt LiNO_3 .

4.2.2 Surface Charge Effects

Utilizing surface charge to encourage the adsorption of specific compounds was one of the first methods that appeared in the literature. The method relies on controlling the electrostatic interactions between the adsorbate and the adsorbent either by altering the chemical environment of the process (usually by fixing the pH at a pre-designed value) or by tailoring the surface of the photocatalyst in a manner that changes its point of zero charge (PZC).

For TiO_2 , the reported PZC is somewhere between pH 6¹⁸ and pH 7.5.¹⁹ This means that pH values higher than 6–7.5 favor the adsorption of positively charged contaminants on TiO_2 , while pH values lower than that disfavor the adsorption of such species. Indeed, a clear pH effect on the photocatalytic reduction of Hg(II) in a mixture prepared by dissolving HgCl_2 and $\text{K}_2\text{Cr}_2\text{O}_7$ was reported.¹⁴

Although the pH primarily affects the adsorption of charged contaminants, it also has a role in the photocatalytic degradation of some of the neutral molecules that tend to dissociate into charged species. In this case altering the pH not only affects the surface charge of the photocatalyst, but also affects the dissociation of the contaminant. This is the reason why the photodegradation rate of formic acid ($\text{p}K_a = 3.75$) peaked at a pH of 3.4.²⁰ Another example is the co-degradation of acetic acid and 2-chlorobiphenyl.²¹ Here, the photodegradation rate of acetic acid peaked at a pH of 4.6, in accordance with its $\text{p}K_a$ (4.7), while that of the neutral species 2-chlorobiphenyl was not affected by changing the pH. The pH effect on dissociation was demonstrated also in the photodegradation of a mixture of 4-hydroxybenzoic acid and benzamide, where the degradation rate of the former was faster than that of the latter at pH 4, whereas the opposite was observed at pH 8.²²

If the photodegradation of neutral molecules leads to the formation of charged species, the pH value will have no more than a slight effect on the degradation rate of the reactants, yet may govern the degradation rate of the intermediates, and eventually the mineralization rate. Indeed, while the photodegradation of 4-chlorophenol was hardly influenced by the pH, its overall mineralization rate was found to decrease abruptly at $\text{pH} > 7$.²³

In general, the degradation of a neutral compound under single contaminant conditions is hardly affected by the pH. This statement is not necessarily correct in the presence of a charged co-solute, where pH changes may affect the degradation rates of both types of molecules due to variation in the role that competitive adsorption plays in the degradation process.²¹

The argument presented above regarding the possibility of using the difference between the solution pH and the PZC of the photocatalyst to obtain specificity explains not only variations in the relative degradation rates of compounds but (to some extent) also provides a reason why a specific TiO₂ photocatalyst is more adequate than another for the degradation of a specific contaminant. For example, differences in the reduction rates of Hg²⁺ between Degussa P25 and Hombikat UV100 were explained by a PZC of 7.1 for the former and 6.2 for the latter.¹⁴ Likewise, the difference in the relative rates of mineralization of acetaldehyde and acetic acid between a sol-gel made TiO₂ film and P25 TiO₂ was found to correlate with variations in the adsorptivity of the two species onto the two types of photocatalysts.²⁴

Overall, although performing the photocatalytic process at a predetermined pH helps to differentiate between positively-charged contaminants and negatively-charged contaminants, the method is of low practicality since it is limited only to charged species and since the level of specificity that can be obtained by the method might be insufficient.

Notably, in parallel to affecting adsorption of charged species, the pH level may affect the degradation kinetics *via* other mechanisms. These mechanisms, for example, include the shifting of energy levels, the altering of the surface OH concentration and the formation of H₂O₂. It is known that the latter may form two hydroxyl radicals *via* homolytic scission.⁸

4.2.3 Overcoating the Photocatalyst

Controlling the surface charge, *en route* to preferential degradation, can be achieved not only by controlling operational parameters like pH, but also by pre-chemisorption of species. Sulfated TiO₂, prepared by reacting H₂SO₄ with Ti(OH)₄, has strong Lewis acid sites. In correlation, the ratio between the mineralization rate constant of heptane to that of toluene was 5.75 for the sulfated titanium dioxide, while for non-sulfated TiO₂, made by calcination of titanium hydroxide, this ratio was no more than 2.7.²⁵

Overcoating may affect adsorption not only by altering surface acidity, but also by altering the polarity of the surface. Titanium dioxide, like many other oxides, shows high adsorption capability for hydrophilic compounds, but is a very bad adsorbent for hydrophobic compounds, including many halo-organics. To overcome this problem, the photocatalyst was overcoated with molecules having hydrophobic moieties that increased the adsorption, and hence the degradation, of hydrophobic contaminants. For example, methyl(trimethoxy)silane chemisorbed on titania was used to increase the degradation of Rhodamine B, which hardly adsorbed directly on the photocatalyst.²⁶ Similar hydrophobic organo-silicone layers were found to be very

efficient in the degradation of the water-insoluble insecticide permethrin²⁷ and in the degradation of the endocrine disrupter 4-nonylphenol.²⁸

Another example of the effect of overcoating is the modification of titanium dioxide nanoparticles with arginine, an electron-donating chelating agent.²⁹ Here, the amino group of the arginine was found to be very efficient in promoting the adsorption of nitrobenzene, leading to faster reductive photodecomposition, compared with un-modified TiO₂.

While grafting organic molecules on the photocatalyst may enhance the photodegradation of hydrophobic contaminants, one should take into account that the grafted molecules are likely to be degraded as well. To overcome this problem it was proposed to coat the photocatalyst with a thin layer of inorganic carbon, produced by thermal carbonization of poly(vinyl alcohol) under an N₂ atmosphere.³⁰ That way, the adsorption of methylene blue was promoted, leading to faster degradation kinetics.

4.2.4 Adsorb & Shuttle

A step forward from overcoating the photocatalyst with an adsorbing layer is to obtain specificity by constructing composite particles made of co-existing photocatalytic domains and inert domains. The basic approach is to use the inert domains as loci for specific adsorption of target molecules that surface-diffuse to the photocatalytic domains following initial adsorption on the inert domains.

While most of the work on the so-called “adsorb & shuttle” approach was aimed at increasing the adsorption of target contaminants without paying much attention to specificity, analyzing the published data reveals that the results definitively imply that the approach can be utilized to obtain specificity, or at least to alter the relative degradation rates in a mixture of contaminants.

One of the simplest (and the earliest) systems demonstrating such possibility consisted of a mixture of activated carbon and titanium dioxide.^{31,32} Here, the synergy effect upon adding carbon was found to depend on the specific compound that was degraded. For example, a synergy factor of 2.4 for 4-chlorophenol, but only 1.3 for 2,4-dichlorophenoxyacetic acid was observed. This difference may provide a means to obtain specificity, in particular when considering the existing variance in the hydrophobicity of commercially available activated carbon materials, originating from their production process.

Thorough work on the photodegradation of propyzamide,³³ propionaldehyde,³⁴ and pyridine³⁵ by various composites, among which were silica, alumina, activated carbon and zeolites was performed by the group of Yoneyama, who even calculated the diffusion coefficient of adsorbed propionaldehyde on the adsorptive substrates.³⁶ It was established that the strength of interaction between the adsorbate and the adsorbent was crucial for the success of the “adsorb & shuttle” approach. Whenever the interaction was weak, the decomposition rate was determined by the amount of adsorbed contaminant, whereas systems showing strong adsorbent–adsorbate interaction not only did not reveal any synergistic effect but in fact were inefficient

due to insufficient mobility that caused the inert domains to apparently act as competitive inhibitors.

Whether adsorption on inert domains leads to an increase or a decrease in the rate of degradation depends not only on the strength of interaction but on the average distance that the target molecules has to cover. For this reason simple mixing of inert activated carbon particles with titanium dioxide particles reduced the degradation rate of Rhodamine 6G (R6G), whereas composite particles having a short diffusion distance exhibited a synergistic effect.³⁷

Achieving long-lasting high specificity with grafted organic molecules that serve to direct adsorption of hydrophobic molecules can be obtained only if measures are taken to protect the grafted molecules, or, otherwise, if the grafted molecules are not directly attached to the photocatalyst surface. In that manner, a composite made of titanium dioxide and silica, grafted with a hydrophobic organo-silane (ormocer), served to degrade phenol, 4-chlorophenol and salicylic acid.³⁸ Of particular importance were the stability tests held for the composite, which showed that the material did not lose its hydrophobicity even after several days of exposure to sunlight. This stability was quite remarkable, taking into account that the average distance traveled was only 7 nm.

While the approach discussed above may significantly increase the photo-degradation rates of contaminants that hardly adsorb on the photocatalyst and may help in preventing the emission of intermediates, its specificity is inherently quite low, as it operates on a class of contaminants, instead of specific target molecules. To increase specificity it was proposed to construct immobile organic molecular recognition sites (MRSs) on inert domains, located in the vicinity of the photocatalyst. These pre-designed recognition sites selectively physisorb target molecules that surface-diffuse from site to site towards the interface between the inert domains and the photocatalytic domains, where they are destroyed (Figure 4.1).

Since the molecular recognition sites are organic, care had to be taken to study the possibility of their destruction by spill-over of oxidizing species

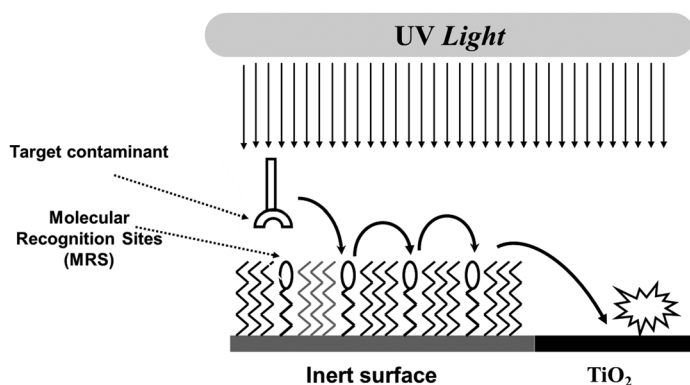


Figure 4.1 Concept of “adsorb & shuttle” using molecular recognition sites.⁴²

formed on the surface of the photocatalyst upon exposure to light. Indeed, it was found that oxidizing species may leave the photocatalyst and might attack organic molecules anchored on oxides as far as 80 (or even 500!) micrometers away from the photocatalytic domains.^{10,12,39,40} This instability was more severe in air than in water, and under 254 nm light than under 365 nm light. A possible mechanism for the remote degradation phenomena could be the formation of H_2O_2 at the surface of the photocatalyst, diffusion of the H_2O_2 to the inert domains and homolytic disintegration of the oxygen peroxide to yield two hydroxyl radicals. Other active oxygen species that were mentioned in this context included atomic oxygen, superoxide radicals and hydroxyl radicals.

The finding that self-assembled monolayers anchored *via* a thiol functional group onto metallic stripes made of gold or platinum were almost totally immune towards remote degradation¹¹ facilitated the development of robust organic recognition sites that can withstand nearby photocatalytic activity. The first system demonstrating this approach used thiolated β -cyclodextrin (β -DC) as the molecular recognition host, and 2-methyl-1,4-naphthoquinone (2MNQ) as the model contaminant.^{41,42} β -Cyclodextrin was chosen based on its torus-like structure containing a cavity of 0.78 nm in diameter, which makes it a size-selective adsorbent.⁴³ The host molecules were chemisorbed on micrometer-sized gold stripes located next to micron-sized titanium dioxide stripes on silicon wafers.

The kinetics of the photocatalytic degradation of 2MNQ on structures made of alternating stripes of titanium dioxide and gold-coated TiO_2 onto which thiolated cyclodextrin had been chemisorbed are shown in Figure 4.2. Each trace depicts the kinetics measured with stripes of different widths, between 5 and 40 μm . In all substrates, the width of the inert stripe was equal to that of the photocatalytic stripe. Degradation of 10%

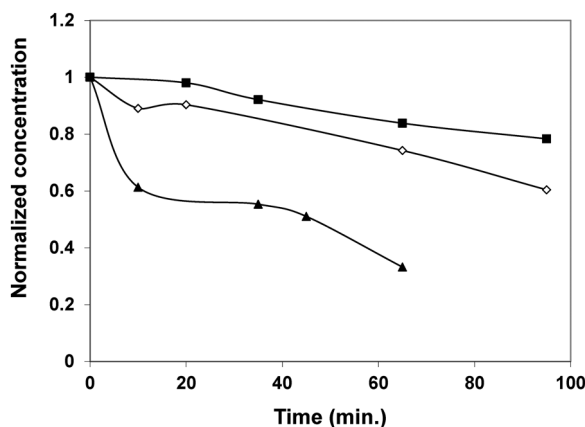


Figure 4.2 Photodegradation kinetics of 2-methylnaphthoquinone on Au-MRS/ TiO_2 stripes of different width. In all samples, the width of the gold stripes was equal to that of the TiO_2 stripes. Width of stripes: (▲) 5, (◇) 20 and (■) 40 μm .⁴¹

of the 2MNQ required approximately 50 min with the 40 μm stripe-width structure, 20 min with the 20 μm stripe-width structure and no more than 5 min with the 5 μm stripe-width structure. In other words, the smaller the domain width, the faster the photodegradation of the 2-methyl-1,4-naphthoquinone, in correlation with reducing the average required distance of diffusion. Notably, no degradation of the thiolated cyclodextrin MRS during the process was observed.

To validate the specificity the degradation rates of 2MNQ and of benzene were compared. Table 4.1 presents the extent of decrease in the concentration of both contaminants following 30 min of exposure, and the ratio between the relative degradation of 2MNQ to that of benzene, for solutions containing one contaminant and for solutions containing a mixture of the two contaminants. Results are presented for substrates made of alternating stripes of gold and titania with and without chemisorbed thiolated cyclodextrin. The effect of the presence of the MRS on the degradation rate, and, more important, on the specificity is clearly reflected in the table. For 2MNQ, the presence of the MRS increased the percentage of degraded molecules for the single contaminant solution by a factor of 3.2 (from 18.7% to 60%) and for the mixed solution by a factor of 1.65 (from 19.8% to 32.6%). The same MRS caused an opposite effect on the degradation of benzene, thus increasing the ratio in the degradation rate of 2MNQ to that of benzene from 0.75 to 8.1 in the single solution experiment and from 0.71 to 4.23 in the mixed solution experiment. The effect of the thiolated cyclodextrin in decreasing the degradation of benzene (which added to the change in the ratio) was explained by the strong interaction between benzene and cyclodextrin.^{44,45}

The same MRS served also to specifically degrade the dye-stuff Chicago Blue Sky 6 (CB).⁴² Here, an aqueous solution containing a mixture of CB and the dye-stuff R6G was exposed to 365 nm UV light. The degradation of the CB dye and that of R6G was calculated based on changes in their UV-VIS spectra, as reflected in their 625 and 527 nm peaks, respectively. It was found that the degradation of the CB was almost twice as fast when using the

Table 4.1 Extent of decrease in the concentration of benzene and 2-methylnaphthoquinone, following 30 min exposure to 365 nm light of vessels containing wafers made of alternating stripes of Au and TiO_2 , with and without MRS. The ratio between the extent of degradation of 2MNQ to that of benzene is also shown.⁴¹

	One contaminant		Two co-existing contaminants	
	Au/ TiO_2	Au-MRS/ TiO_2	Au/ TiO_2	Au-MRS/ TiO_2
Decrease in 2MNQ concentration (%)	18.7	60	19.8	32.6
Decrease in benzene concentration (%)	25	7.4	28	7.7
Ratio 2MNQ:benzene	0.75	8.11	0.71	4.23

MRS-containing samples. This enhancement was not observed for R6G. It was suggested, albeit not proved, that the enhancement in the photodegradation of Chicago Blue was closely related to its structure of two interconnected “legs” made of conjugated aromatic rings. Each cyclodextrin cavity can accommodate no more than part of one “leg” so that the rest is out of the cavity and may physisorb on a second β -CD site.

A second molecular recognition system used to obtain specificity was based on Cu^{2+} ions replacing the protons in two adjacent chemisorbed 1,1-mercaptopoundecanoic acid (MUACu) molecules.⁴⁶ This system was designed for the photodegradation of diisopropyl methylphosphonate (DIMP), known as a simulant for the nerve agent sarin. Similar to the previous case, the measurements were performed on silicon wafers coated with alternating microstripes of photocatalytic titanium dioxide and inert gold substrates, onto which the MRSs were chemisorbed.

The evolution of the IR spectrum during a typical photocatalytic experiment is presented in Figure 4.3(a)–(e). Typical DIMP peaks are observed at 917, 990, 1108, 1263 and 2982 cm^{-1} . The changes in the spectrum correlate well with the degradation of DIMP, the formation of acetone (1735, 1367 and 1212 cm^{-1}) as an intermediate product, and the formation of CO_2 (2348 cm^{-1}) and water as the final products. This process occurred simultaneously with desorption of DIMP from the reactor’s walls, which partially compensated for the loss of DIMP from the gas phase. The evolution of the spectra in experiments with patterned substrates that had not been previously coated with MUACu was qualitatively similar. Control experiments indicated that

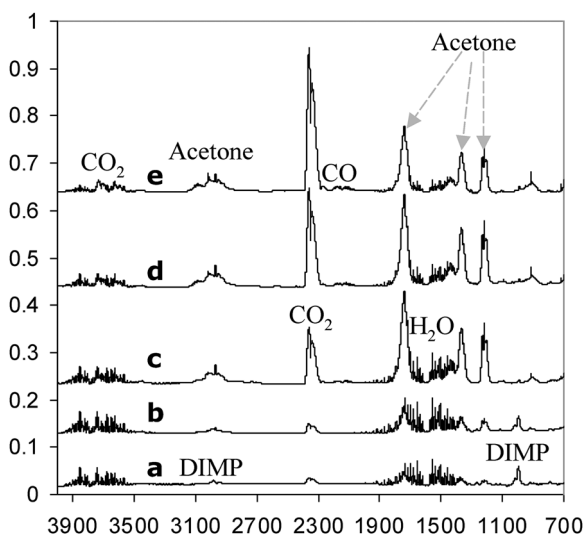


Figure 4.3 Evolution of an FTIR spectrum (cm^{-1}) upon photodegradation of DIMP (diisopropyl methylphosphonate) on $\text{TiO}_2/\text{MUACu}$: (a) before UV exposure, (b)–(e) following UV exposure for 3, 19, 39, 60 h, respectively.⁴⁶

the degradation of DIMP was due to photocatalysis and not due to direct photochemistry.

The effect of the MUACu MRS on the photodegradation of DIMP is demonstrated in Figure 4.4, which shows the kinetics of formation and disappearance of acetone for both types of substrates. Results were presented in a manner that normalized the amount of acetone according to the maximum amount of measured acetone. As depicted in the figure, the rate of production of acetone in the presence of MUACu domains, measured during its rise in concentration, was higher by a factor of 2.5 than that observed with samples containing the same photocatalytic surface area but without MUACu. Similarly, examination of the production of CO_2 in these two systems revealed a faster increase in the mineralization rate for the MUACu-containing system, albeit by a factor of less than three. Exposure of DIMP to these two systems in the dark did not yield any significant amounts of acetone or CO_2 , despite the fact that Cu^{2+} and some of its chelates may act as hydrolyzing catalysts for phosphonates.

To find out whether the above-described enhancement in the quantities of the intermediate product acetone in the MRS-containing system was due to enhanced degradation of DIMP by the MUACu or due to slower photodegradation of acetone, the photodegradation of acetone was measured with various substrates. These substrates included structures made of alternating stripes of gold and TiO_2 , alternating stripes of MUACu-coated gold and TiO_2 and thin films of titanium dioxide without any metal stripes. For all structures, a first order reaction with the same rate constants was measured, demonstrating that the presence of MUACu or gold did not have any effect on the rate of acetone photodegradation. Hence, it was concluded that this structure enhanced specifically the degradation of DIMP but not that of acetone.

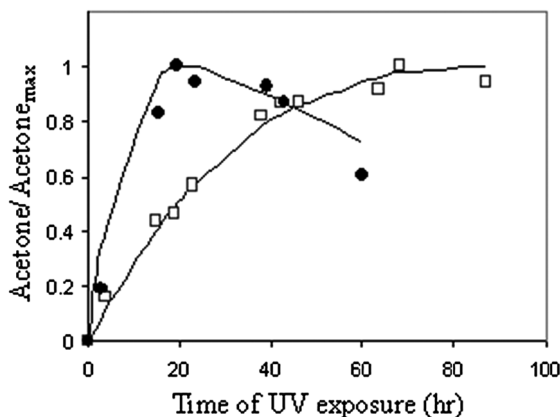


Figure 4.4 Kinetics of acetone production during photodegradation of DIMP. (□) TiO_2/Au stripes (5 μm in width) without the MUACu MRS; (●) TiO_2/Au stripes (5 μm in width) with the MUACu MRS.⁴⁶

To quantify the benevolent effect of the “adsorb & shuttle” approach, the results were modelled, while taking into account reversible adsorption of DIMP on the reactor’s walls:



According to the kinetic model the ratio of the concentrations of acetone to the maximal concentration of acetone is given by:

$$\frac{[\text{Acetone}]}{[\text{Acetone}]_{\text{max}}} = \frac{k_1}{k_3 - k_1} \left[\frac{k_3}{k_1} \right]^{k_3 - k_1} \left[e^{-k_1 t} - e^{-k_3 t} \right] \quad (4.3)$$

By taking k_3 as the rate constant measured for the degradation of acetone, the authors were able to calculate k_1 , the rate constant for the photocatalytic degradation of DIMP. Values of 0.1 and 0.01 h^{-1} were calculated for a system containing the MRS and for the control system, respectively. This reflected an improvement in k_1 by a factor as large as 10 due to the presence of the molecular recognition sites.

Unlike the thiolated β -cyclodextrin system, some degradation of the organic part of the MRS upon irradiation was observed. XPS measurements suggested that, in this case, the thiol part of the MRS remained attached to the metal and was connected directly to the copper ion, which served to physisorb the DIMP molecule. Indeed, repeated measurements revealed that despite this loss in activity the performance of the MRS-containing system was still significantly better than that of fresh TiO_2 (Figure 4.5).

The fact that the benevolent effect of the MUACu was noticed with DIMP, but not with acetone, evidently showed that MRS may serve not only to increase degradation rates but also to induce preferential photodegradation. Such specificity is of great importance in particular in systems where the intermediate products are far less hazardous than the initial reactants (as in the case of sarin).

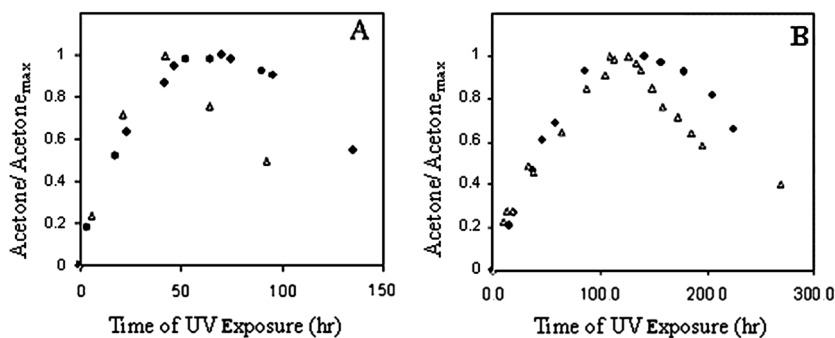


Figure 4.5 Ratio of acetone concentration at a given time and its maximum value during DIMP photodegradation on (A) (Δ) fresh $\text{TiO}_2/\text{Au} + \text{MUACu}$; (\bullet) reused $\text{TiO}_2/\text{Au} + \text{MUACu}$; (B) (Δ) fresh TiO_2 ; (\bullet) reused TiO_2 .⁴⁶

The enhancement in degradation rate is expected to become more pronounced as the average required length of diffusion becomes shorter. Nevertheless, shortening the distance that the contaminants have to pass means also that the anchored MRSs are more prone to attack by oxidizing species formed at the surface of the photocatalyst. It is therefore expected to have an optimal domain size. The optimal size should depend on the medium (liquid phase *versus* gas phase) and on the diffusion coefficient of the contaminant on the MRS “substrate”.

4.2.5 Doping

Another way to achieve preferential degradation through controlling adsorption is by using surface dopants. Good candidates are lanthanides, known to form complexes with acids, amines, aldehydes, alcohols and thiols. Indeed, doping TiO_2 with lanthanides had a significant effect on the photodegradation rate of *p*-chlorophenoxyacetic acid.⁴⁷ The specific interaction between the dopant and the acid affected the distribution of intermediates, as the only intermediate that was found was *p*-chlorophenol, instead of hydroquinone and chloroquinone that had been found in the case of pure TiO_2 . Another example is the loading of nanoclusters of silver ions that positively affected the photocatalytic reduction of bis(2-dipyridyl)disulfide (RSSR) to 2-mercatopyridine, due to enhanced adsorption of RSSR.⁴⁸

An interesting example of the effect of dopants in promoting specific adsorption, leading to faster photocatalytic degradation, was reported with BiOCl .⁴⁹ Here, a comparison was made between pristine BiOCl , Fe-doped BiOCl , Nb-doped BiOCl , Fe,Nb co-doped BiOCl , In,Nb co-doped BiOCl and La,Nb co-doped BiOCl . The kinetics of adsorption of Rhodamine B (RhB) under dark conditions on these photocatalysts is presented in Figure 4.6. The $\text{BiOCl}(\text{Fe},\text{Nb})$ compound revealed extraordinary high adsorption capability towards RhB (more than 70%). In contrast, the other five compounds hardly adsorbed the RhB under these conditions. The specific surface area did not play any role since all compounds had a similar specific surface area. The difference in the adsorption behavior is in particular interesting since one may expect that lack of adsorption on each of the single dopant-containing substrates might predict lack of adsorption also in a system containing both dopants.

The effect of co-doping with Nb and Fe on the adsorption of other species, such as salicylic acid, was not observed, demonstrating the importance of dopants for specific adsorption. It was proposed that in this case the high adsorptivity had to do with the known tendency of iron ions to form complexes with rhodamine.⁵⁰

The specific adsorption on the surface of the photocatalyst had an impact on the photocatalytic kinetics. The apparent rate constants obtained for BiOCl , $\text{BiOCl}(\text{Fe})$, $\text{BiOCl}(\text{Nb})$, $\text{BiOCl}(\text{La},\text{Nb})$, $\text{BiOCl}(\text{In},\text{Nb})$ and $\text{BiOCl}(\text{Fe},\text{Nb})$ were 0.0168, 0.0258, 0.026, 0.0221, 0.0273 and 0.091 min^{-1} , respectively.

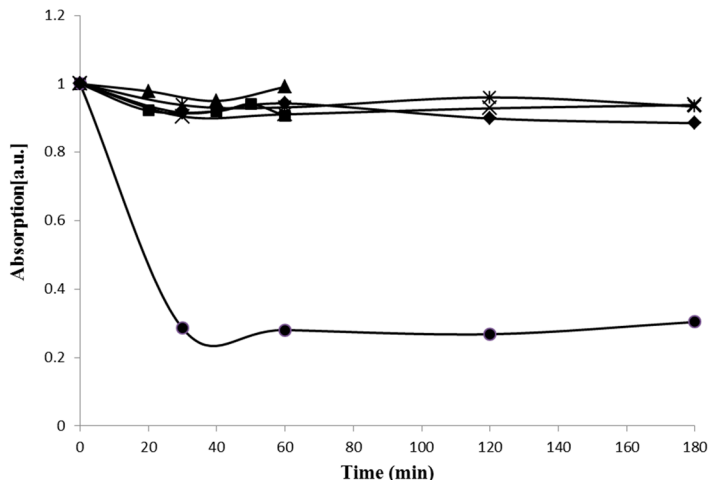


Figure 4.6 Adsorption of RhB in the dark on as-synthesized BiOCl (×), BiOCl(Fe) (■), BiOCl(Nb) (▲), BiOCl(Fe,Nb) (●), BiOCl(In,Nb) (◆), BiOCl(La,Nb) (*).⁴⁹

As expected, the rate constant with TiO_2 and the rate constant in the absence of a photocatalyst were negligible.

Evidently, the presence of dopants had a dramatic effect on the photocatalytic degradation rates of the dye. Here, the photo-activity of all three doped systems was higher than that of the un-doped BiOCl; the (Fe,Nb)-doped system being significantly more active than the rest. Notably, the difference in kinetics was less pronounced when UV light was used. The difference between exposure to UV light *versus* exposure to visible light in the synergistic effect was explained by the sensitivity of the degradation mechanism under visible light (sensitization by the dye molecule, followed by charge transfer from the dye to the semiconductor and formation of superoxide anions) to the strength of the interaction between the adsorbate and adsorbent. In contrast, the mechanism under UV light (photocatalysis *via* formation of OH radicals) was less affected by the strength of the interaction between the dye and the substrate.

4.2.6 Selection by Size

Selection by size is a well-known mechanism in the area of thermal catalysis, most notably by the use of zeolites. Utilization of this mechanism in photocatalysis should not be taken as trivial, due to the extra requirements originating from the need to match the contaminants and the photocatalytically-generated active species. One of the first examples of this approach was the incorporation of titanium dioxide into sheet silicates of clay, using the distance between adjacent layers in the clay as a filter that enhanced the photodegradation of molecules smaller than the interlayer distance.⁵¹ That way,

small carboxylic acids (up to C_8) were degraded by the composite structure faster than with TiO_2 powder, whereas capric acid (C_{10}) was found to degrade faster by TiO_2 powder than with the composite clay photocatalyst.

Increasing selectivity (and actually also activity) was obtained by treating a microporous titanosilicate photocatalyst with HF. A complete abatement of 2,3-dihydroxynaphthalene (DHN) co-existing with phenol in a solution was observed within 10 min, whereas the degradation of phenol was minute. Apparently, the zeolitic internal cavities offered a protective environment against degradation for species that can easily diffuse inside. Another possibility was that the size selectivity in this case was governed by the ability of the photocatalyst to accommodate contaminants in the vicinity of the pore mouth.⁵² In a similar manner, grafting of titanium dioxide onto the pore surface of mesoporous silicates was found to enhance the degradation rate of α -terpinol by a factor of 4 compared to P25, but reduced the degradation rate of the dye Rhodamine-6G by a factor of 2.⁵³

4.2.7 Molecular Imprinting

Imprinting the target molecules on the surface of the photocatalyst during the preparation of the latter is an excellent way to combine high specificity with high stability (Figure 4.7). The method is heavily in use for sensing, utilizing mostly polymeric matrices, but also sol-gel oxides, in particular silica.^{54,55} The use of imprinted TiO_2 is not very common; nevertheless, one may find quite a few works on imprinting on titania, again, mostly for analytical purposes.^{56,57} For a review on imprinted TiO_2 see Nussbaum and Paz.⁵⁸

Unlike sensing, not much is found in the literature on the use of imprinted titanium dioxide for the purpose of photocatalytic decontamination of air or water. This can be explained, at least partially, by the high temperatures required for the phase transition from the amorphous inactive phase, obtained by common sol-gel procedures, to the photoactive anatase phase (>300 °C). Such high temperatures might harm the system by premature evaporation (or even burning) of the organic guest molecule. To overcome the anatase-phase obstacle, three main strategies were developed: (1) utilizing specific methods for TiO_2 formation that do not require high temperatures, like the titanyl-sulfate method (Figure 4.7A, denoted as MI),⁵⁹ (2) overcoating a core of pre-prepared crystalline TiO_2 particles by an imprinted polymer (Figure 4.7B, denoted hereby as MIP)⁶⁰ and (3) imprinting on a thin inorganic (usually silica) shell, overcoating anatase phase particles, defined hereby as MII (Figure 4.7C).^{61,62} A fourth approach for imprinting, which is in use in sensors but not in photocatalysis, is imprinting a molecule on the photocatalyst, and using this molecule without removing it as a host for the target molecule (Figure 4.7D).

A viable possibility, related to approach (1) is the construction of an amorphous (or even a crystalline) imprinted TiO_2 layer on top of highly efficient, commercially-available TiO_2 particles. This approach was first demonstrated

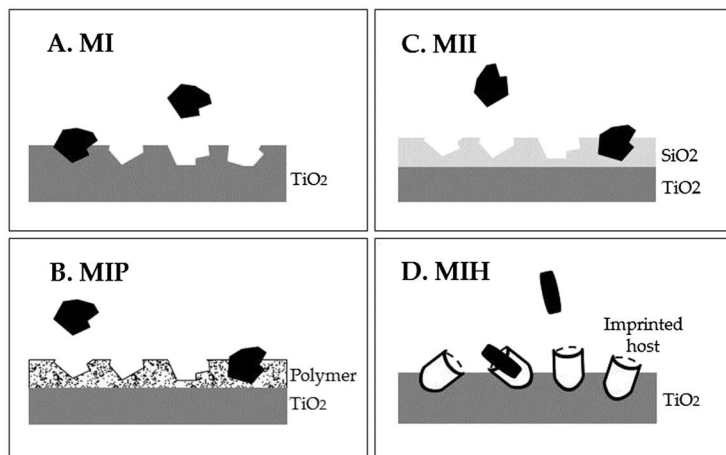


Figure 4.7 Four types of TiO₂-imprinted devices: (A) molecular imprinting on TiO₂ (MI), (B) molecular imprinting on a polymer shell overcoating a TiO₂ core (MIP), (C) molecular imprinting on an inorganic shell overcoating a TiO₂ core (MII), and (D) molecularly imprinted host (MIH).⁵⁸

by imprinting salicylic acid on thin films formed by liquid phase deposition (LPD) on P25 particles.⁶² Similarly, a “layer by layer” (also called “dipping–rinse–hydrolyzation”) technique was utilized by imprinting anthracene-9-carboxylic acid (9-AnCOOH) on ultrathin TiO₂ films grown on TiO₂ nanotube arrays.⁶³

Removal of the imprinted molecule is performed by dissolving (*e.g.*, in a dilute solution of ammonia), by burning out the organic guest or simply by photocatalytic degradation. In terms of efficiency ratio the latter method was found to yield the best results, at least for salicylic acid.⁶² Typical efficiency ratios in the literature range between 1.5 and 9.2.⁵⁸

Defining the preferentiality factor as the ratio between the efficiency ratio for the target molecules divided by the efficiency ratio for a foreign molecule one gets typical values that range between 2 and 6, depending on the type of targets and guests and on the geometrical and chemical similarity between the targets and the guests. In the case of a series of nitrophenols it was found that the preferentiality factor depended not only on the chemical difference between the target and the non-target molecules but also on the concentration of the target molecule.⁶³ An exceptionally high preferentiality factor (8.7–12.2) was observed upon imprinting diethyl phthalate and comparing its degradation rate on the imprinted photocatalyst *versus* that of phenol.⁶¹

Accepting the fact that imprinting increases the degradation rate of the imprinted molecules raises an interesting question regarding a possible negative effect on the rate of degradation in the presence of co-existing molecules. In this context, the degradation rate of 2-nitrophenol that had been imprinted on a polymer-overcoating titania changed dramatically upon varying the co-existing molecules. For example, the rate constants in the presence of 2,4-dinitrophenol was ten-times smaller than the rate constant

measured in the presence of toluene.⁶³ Another interesting question is the effect of imprinting on the degradation rates of co-existing molecules. Here, the presence of cavities of 2-nitrophenol induced a decrease in the degradation rate of toluene and naphthol (which are structurally very different from 2-nitrophenol), but increased the degradation rate of 2,4-dinitrophenol and phenol (which are structurally similar to 2-nitrophenol).⁶³ Similarly, the degradation rate of the sarin-simulant di-isopropyl methylphosphonate (DIMP) on titanium dioxide particles, prepared by the titanyl sulfate method and imprinted with diethyl-hydroxy-methylphosphonate (DEHMP), was found to be faster than that observed upon imprinting DIMP.⁶⁴ The enhanced performance of the DEHMP-imprinted photocatalyst was likely due to its hydroxyl group, which facilitated stronger interaction with the TiO₂ precursor.

These two cases represent an approach in molecular imprinting where instead of imprinting the target molecules one imprints the so-called pseudo-target molecules. The pseudo-target molecules are characterized by a geometrical structure that is similar to that of the target molecules and by an ability to form good interactions with the photocatalyst's precursor. The use of pseudo-target molecules should be considered whenever the interaction between the target molecule and the photocatalyst's precursor is problematic or if the target molecules are too toxic or too expensive.

The selectivity obtained by imprinting pseudo-targets was modeled for the degradation of a mixture containing both the target molecules and the pseudo-targets.⁶⁰ The model was basically a typical enzyme-substrate model, where the pseudo-guest's cavities were represented by the enzyme, the target molecules replaced the substrate and the pseudo-guest molecules were considered as reversible non-competitive inhibitors. A very good correlation was observed with this double reciprocal (Lineweaver-Burk) kinetics representation.

Notably, obtaining high specificity requires that the relative area covered with the imprinted cavities would be as high as possible. Increasing the concentration of the imprinted molecules during the preparation of the photocatalyst may assist in achieving this goal. However, increasing the concentration of the imprinted molecules might increase the chances for the appearance of interconnected cavities and aggregates that are likely to reduce specificity.

As mentioned above, under LH kinetics, one may expect a direct correlation between increasing the adsorbability of the target molecules and increasing the rate of degradation. To check the validity of such correlations we have calculated the adsorption ratio (*i.e.* the ratio between the adsorption of the target molecule on the imprinted substrate and its adsorption on a non-imprinted photocatalyst). In parallel, the rate ratio (*i.e.* the degradation rate constant on the imprinted substrate and the degradation rate constant on a non-imprinted photocatalyst) was calculated. The data, compiled from various sources, appeared in a previously published review⁵⁸ and is presented in Figure 4.8. The figure presents results for photocatalysts imprinted with chlorophenols,⁶⁵ nitrophenols,⁶⁶ diethyl phthalate,⁶¹ salicylic acid,⁶² DIMP⁶⁴ and DEHMP.⁶⁴ Here, the *x*-axis represents the adsorption ratio whereas the *y*-axis represents

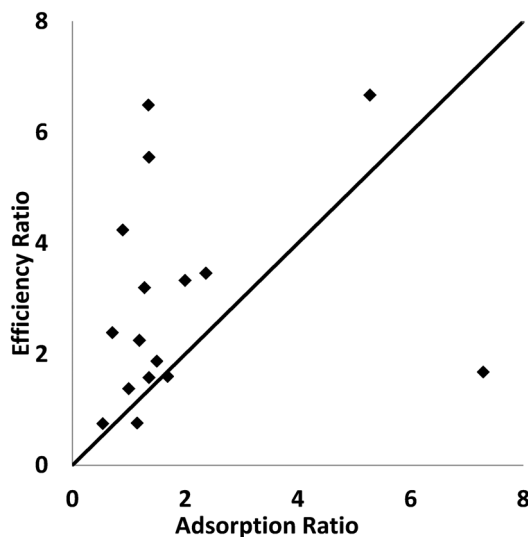


Figure 4.8 Rate (efficiency) ratio *versus* adsorption ratio for various imprinted molecules including chlorophenols, nitrophenols, diethyl phthalate, salicylic acid, DIMP and DEHMP. The straight line represents an imaginary situation where the efficiency ratio is equal to the adsorption ratio.

the efficiency ratio. The straight line represents an imaginary situation where the efficiency ratio is equal to the adsorption ratio. From the figure it is evident that almost all the data points are located to the left of this line. This means that the effect of imprinting on the photocatalytic activity surpasses the effect of imprinting on adsorption. The higher effect of imprinting on the degradation rates may be explained by a better coupling between the adsorbed molecules and the photocatalyst surface. It is known that good coupling between the adsorbed molecule and the surface of the photocatalyst increases the odds for direct oxidation by holes.⁶⁷ In that case, the rates are expected to increase not only due to the presence of a second mechanism operating in parallel, but also because a direct mechanism utilizes the larger oxidation potential of the holes relative to that of hydroxyl radicals.

An exception was observed in the degradation of anthracene-9-carboxylic acid in TiO₂ nanotubes imprinted by the “dipping–rinse–hydrolyzation” (DRH) method.⁶³ Here, the adsorption increased by a factor of 8.8 whereas the increase in the reaction rate was no more than 1.5. This may reflect a situation where many of the imprinted adsorbing sites are photocatalytically inactive. The inactivity could stem from blocking of the space between adjacent nanotubes or simply because the length of the tubes was far longer than the light penetration depth. The fact that the adsorption on the thick layer photocatalyst was better than on the thin layer photocatalyst, yet the photocatalytic activity with the thick layer photocatalyst was worse than with the thin layer photocatalyst seems to support this explanation.

Two important issues *en route* for large-scale implementation of imprinting are repeatability and stability. Repeatability tests with imprinted substrates

prepared by liquid phase deposition of TiO_2 on P25 were performed taking salicylic acid as the target molecule.⁶² It was found that 97% of initial photocatalytic activity remained after six successive runs, each of which lasted for 180 min of exposure followed by washing with water to remove residual salicylic acid and byproducts. Likewise, the photo-electrocatalytic efficiency in the degradation of anthracene-9-carboxylic acid by imprinted ultrathin layers grown on TiO_2 nanotube arrays was found to decrease by no more than 2.5% after ten 30 min cycles of reaction.⁶³ High stability was observed also in the degradation of diethyl-phthalate imprinted on MII particles.⁶¹

Unlike imprinting on an inorganic matrix, imprinting on a polymer (as in the MIP approach) is prone to loss in specificity, due to inevitable damage to the polymeric matrix. Using robust polymers (polyaromatics, for example) or introducing sacrificial agents may assist in circumventing this problem; however, full success cannot be guaranteed.

4.3 The Redox Reaction

Although controlling the adsorption is the most common way to obtain specificity, it is possible to regulate the relative photocatalytic degradation of species by taking advantage of the mechanism of the redox reaction. This can be done, for example, by controlling the type of the active species. Controlling the type of active species can be achieved by altering the location of the conduction band and valence band of the photocatalyst or by using sensitizers. While the level of specificity to be obtained is not expected to be high, it is still a viable route in specific cases.

4.3.1 Recombination *Versus* Interfacial Electron Transfer

Large variations (3–10) in the ratio between the degradation rates of 1,2-diphenylhydrazine to that of benzidine upon using P25, Hombikat UV100 and Millennium PC500 were observed.⁶⁸ It was claimed that these variations had to do with the fact that some photocatalysts (P25, for example) owed their activity to a slow recombination rate, whereas others (UV100, for example) revealed high activity due to fast interfacial electron-transfer rate.⁶⁹ As a consequence, P25 may be more adequate for the degradation of molecules when their adsorption is slow, whereas UV100 is more adequate for molecules when their adsorption (and desorption of intermediates) is relatively fast.⁶⁸ This provides a way to control specificity.

4.3.2 Doping as a Means to Control Oxidation *Versus* Reduction

It is well established that doping by noble metals, such as Pt or Pd, may accelerate the cathodic process of oxygen reduction.⁷⁰ While the main effect is that of reducing recombination rates, and hence increasing the rates of both oxidation processes and reduction processes, a secondary effect, related to

the elevated concentration of superoxide anions, may alter the relative rates of degradation between organic compounds, thus providing a means to control specificity. In such manner, metallization increased the degradation rate of methanol and ethanol, which degrade through oxidation, but reduced the degradation rate of trichloroethylene, chloroform and dichloropropionic acid (DCP).⁶⁷ Likewise, doping with V(IV) increased de-chlorination of carbon tetrachloride relative to degradation of chloroform (*i.e.* reduction relative to oxidation), whereas doping with Ru(III) had the opposite effect.⁷¹ Another example is the effect of doping Hombikat UV100 with platinum, where the photodegradation ratio between dichloroacetic acid (DCA) and 4-chlorophenol was found to increase two-fold following doping.⁷²

Silico-tungstic acid (STA = $\text{H}_4\text{SiW}_{12}\text{O}_{40} \cdot n\text{H}_2\text{O}$) is a multi-electron redox agent, which can interact with photogenerated electrons and holes. It was found that modifying TiO_2 with STA led to preferential degradation of nitroglycerine relative to that of co-existing ethanol or acetone. Platinization of the photocatalyst yielded the opposite effect. In that manner, preferential degradation was achieved, albeit at the expense of reducing the overall photocatalytic activity.⁷³

4.3.3 Shifting the Location of Energy Bands

As mentioned above, a clay matrix, into which titanium dioxide was embedded, was found to be quite efficient in promoting the degradation rates of small carboxylic acids relative to that of larger acids.⁵¹ While the mechanism explaining this phenomenon was claimed to be related to the interlayer distance, the authors still considered a possibility that a shift in the location of the bottom of the conduction band of the embedded titanium dioxide particles was responsible for the observed specificity.

4.3.4 Co-Existing Compounds as a Means to Alter Specificity

It is known that certain molecules are photocatalytically degraded *via* the formation of highly active radicals that may induce reactions in other organic compounds. Since the extent by which the highly active radicals affect the second compound varies from one compound to the other, it is possible to use this phenomenon to alter relative degradation rates.

The best example of this approach is probably trichloroethylene (TCE). It was found that, under dry conditions, addition of TCE increased the rate of photocatalytic degradation of organic compounds, most likely due to the presence of chlorine radicals, formed in the photocatalytic degradation of gas-phase TCE. These radicals were also considered to be the source of the very high quantum yields reported for the photodegradation of gas-phase TCE.⁵ At the same time TCE also competed on adsorption sites with the co-existing organics. The net effect varied from one compound to another. In this way, the presence of TCE increased the rate of degradation of *i*-octane,⁷⁴

toluene, *m*-xylene and ethylbenzene⁷⁵ but had a negative effect on the degradation rate of benzene⁷⁵ and methanol.⁷⁶ Hence, the presence of gas-phase TCE may act to alter the relative rates of degradation.

4.3.5 Utilizing Specific Adsorbate–Adsorbent Interactions

The degradation of dyes is often characterized by the emission of stable intermediate products that, depending on exposure time, may further degrade. In general, several reaction mechanisms may operate in parallel, so that at each point in time the distribution of intermediates depends on the relative importance of each mechanism and on its reaction coordinate. Various factors may govern the relative importance of a specific mechanism, among which is the way by which the adsorbate is attached to the surface of the photocatalyst. Therefore, modifying the photocatalyst in a manner that alters the functional group responsible for binding is expected to influence the distribution of products. In many cases, the effect is coupled with the ability of the dye molecules to act as sensitizers, *i.e.* to inject charges into the semiconductor upon excitation. In that case, the distribution of intermediate products may be wavelength-dependent.

As an example, one may consider the photo-assisted oxidation of the dye Rhodamine B.⁷⁷ At pH 4 the surface of TiO₂ is positively charged, so that the dye weakly adsorbs through its negatively-charged carboxyl group. In contrast, adsorption on a SiO₂–TiO₂ composite photocatalyst takes place by the positively-charged diethylamino group. Consequently, visible-light induced degradation with the composite photocatalyst was characterized by a highly selective stepwise *N*-de-ethylation process prior to the destruction of the chromophore structure, whereas on TiO₂ (P25) destruction of the chromophore took place prior to *N*-de-ethylation.

4.3.6 Surface Derivatization

Derivatization of the photocatalyst can be applied not only to control adsorption of reactants but also to govern the distribution of products by virtue of controlling the mechanism of degradation. As an example, TiO₂ nanoparticles were derivatized with Fe(III)-porphyrin and were exposed to UV light in the presence of alkanes and alkenes.⁷⁸ The bonded porphyrin enhanced the yield and formation rate of mono-oxygenated products with respect to the formation of CO₂. In addition, the grafted porphyrin also increased the alcohol to ketone ratio. Results were explained by the opening of a second avenue for degradation, based on reduction of the ferric porphyrin, leading to reductive activation of O₂ bound to the porphyrin. This activated porphyrin complex may react with oxidatively pre-formed alkyl radicals to give an alcohol that easily disconnects from the porphyrin (Figure 4.9). Hence, in this case the porphyrin served not only to open a new route for reaction but also to promote desorption of intermediates. Notably, during the degradation process

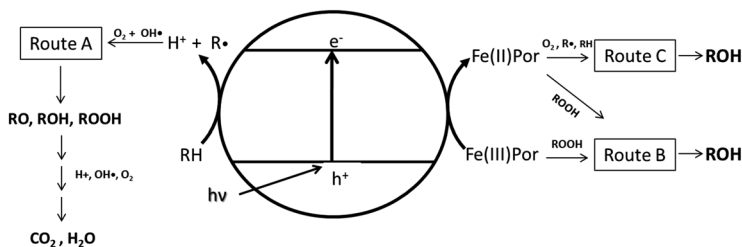


Figure 4.9 Schematic representation of the photo-oxidation mechanism of cyclohexane on Fe(III)-porphyrin surface modified TiO_2 .⁷⁸

the grafted porphyrin showed remarkable stability despite its organic nature. This high stability is of high value whenever the use of grafted molecules is considered.

4.3.7 Sensitization as a Means to Induce Specificity

Sensitization of photocatalysts – *i.e.* absorption of light by dye molecules bound to a semiconductor, followed by charge injection leading to the formation of active species on the surface of the semiconductor – has been documented since the early days of photocatalysis. Two main factors governing the efficiency of the process are the strength of binding between the dye and the semiconductor and the coupling between the absorption spectrum of the dye and that of the impinging light. This can be used to induce not only preferential degradation of dyes but also to gain some control over the emitted products.

In this context it has been shown that the degradation rate of 2,4,5-trichlorophenol, which forms a charge transfer complex with TiO_2 , is correlated with its absorption spectrum.⁷⁹ In principle, this can be utilized to differentiate between contaminants in a mixture, simply by using a narrow-band irradiation and by choosing a photocatalyst that specifically forms a charge-transfer complex with the target contaminant. This suggestion should be taken with a grain of salt since in some cases the correlation between the action spectrum and the absorption spectrum of the dye can be quite weak.⁸⁰ This weak correlation between the absorption spectrum of the dye and its action spectrum could stem from the fact that the parameter usually taken in the literature for this correlation is the absorption spectrum of the dye in solution instead of the absorption spectrum of the adsorbed dye.

Figure 4.10 presents changes in the absorption spectrum of Rhodamine B upon exposure to broad band visible light.⁸¹ As presented in the figure the degradation is characterized by a decrease in the absorption of the solution at 544 nm, representing the destruction of the chromophore, and by the appearance of a broad peak at a lower wavelength, typical for partially *N*-de-ethylated Rhodamine B. A clear difference between the spectrum that was obtained with a BiOCl photocatalyst and that with $\text{La}_2\text{BiNbO}_7$, is observed,

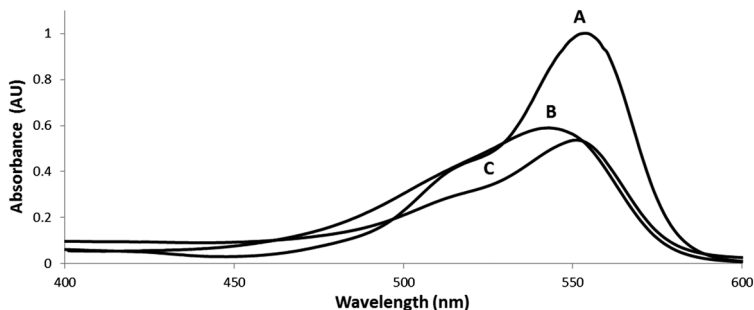


Figure 4.10 (A) Spectrum of Rhodamine B (RhB) prior to degradation, peaked at 554 nm. (B) and (C) degradation of RhB with BiOCl (B) and with $\text{La}_2\text{BiNbO}_7$ (C) under visible light. Traces (B) and (C) present the spectrum at a point where 48% of the initial absorbance at 554 nm has disappeared.⁸¹

reflecting the effect of the catalyst on the distribution of products and in particular the effect on the ratio between *N*-de-ethylation *versus* the degradation of the chromophore.

4.4 Desorption of Products

Desorption of intermediate and final products plays a symmetrical role to that of the adsorption of the reactants. As part of this symmetry, difficulties in desorption of intermediate products are expected to alter product distribution and, in particular, to decrease the emission of stable intermediates. This was manifested, for example, in the photodegradation of benzene on TiO_2 and on a composite material containing TiO_2 and pillared clays (mica, montmorillonite and saponite), where the different relative desorption of products altered the distribution of end-products.⁸² Likewise, the use of composite particles made of P25 and activated carbon totally prevented the appearance of any intermediates in the photodegradation of gas phase TCE.⁸³

It is well-known (but overlooked to some extent) that certain contaminants (in particular aromatics) might leave behind end-products that are strongly adsorbed on the photocatalyst, thus hindering the photocatalytic activity. It is sensible to assume that this deleterious outcome might affect not only the rate of degradation but also specificity. Yet, as far as we know, the literature is silent with respect to such effects.

4.4.1 Preferential Desorption from Imprinted Photocatalysts

The geometrical compatibility between the contaminant and the photocatalyst may play an important role in preventing desorption of bulky byproducts. In contrast, small molecules such as carbon dioxide may desorb easily due to a combination of low adsorption energy and weak entropic barrier.

Indeed, the accumulated levels of 3-nitrocatechol and 1,2,4-benzenetriol produced during the degradation of 2-nitrophenol were lowered significantly in imprinted TiO₂. Likewise, smaller amounts of benzenetriol were released in the degradation of 4-nitrophenol.⁶⁶

The ability to reduce the emission of intermediates is in particular important in cases where the intermediate products are highly toxic. A good example is the photocatalytic degradation of diethyl phthalate (DEP) on TiO₂ overcoated with a thin layer of imprinted SiO₂.⁶¹ Here, a comparison with a mixture of TiO₂ particles and silica particles revealed a significant reduction in the accumulation of the toxic aromatic byproducts phthalic acid and diethyl 2- and 3-hydroxyphthalate.

The use of pseudo-templates (molecules that geometrically resemble the target molecules, yet with a good affinity to the photocatalyst's precursor) may also affect the distribution of intermediates and end-products. *p*-Chloranil and tetrachlorohydroquinone (TCHQ) are usually found during the photocatalytic degradation of pentachlorophenol (PCP) over P25. In contrast, degradation of the same contaminant on TiO₂, overcoated with a polymer that had been imprinted with 2,4-dinitrophenol (DNP) cavities, did not release any intermediates, probably due to some interaction between the PCP molecules and amino groups in the footprint cavities.⁶⁰ Notably, the degradation of DNP on DNP-templated particles released the same species found during the photocatalytic oxidation of DNP on P25 (albeit in smaller concentration), thus pointing to the potential use of pseudo-templates not only to reduce the concentration of intermediates but also as a tool to direct photocatalytic reactions towards preferred products.

4.4.2 Effect of Solvents on the Desorption of Intermediate Products

As mentioned above (Section 4.2.1), altering the solvent used during photocatalytic degradation may serve as a means to affect specificity by modifying the tendency of the reactants to be adsorbed on the surface of the catalyst. By the same token, the solvents may also affect the desorption-adsorption balance of intermediate products, and therefore may be used to control the distribution of end-products. As an example, one may take the photo-assisted mono-oxygenation of cyclohexane to C₆H₁₀O and C₆H₁₁OH in a set of C₆H₁₂/CH₂Cl₂ mixtures.⁸⁴ Increasing the content of methylene chloride enhanced the formation of mono-oxygenated products and decreased the production of CO₂. This was attributed to an increase in the desorption rate of the alcohol intermediate. Further control of the C₆H₁₀O to C₆H₁₁OH ratio was obtained upon introducing the electron scavenger C(NO₂)₄ into the system. Here, the net result was an increase in the ratio of the production rate of the alcohol to that of the ketone.

Solvent effects on the distribution of products were also found in the photocatalytic reduction of CO₂ with a CdS photocatalyst.⁸⁵ Here, the ratio

between the end-products formate and carbon monoxide was found to increase with the dielectric constant of the solvent. The key factor in this effect was claimed to be the ability of the solvent to dissolve $\text{CO}_2^{\cdot-}$ anion radicals. These radicals are poorly solvated in low polar solvents such as CCl_4 or CH_2Cl_2 , and hence tend to strongly adsorb on Cd sites if such solvents are used. This leads to the formation of CO as the major reduction product. On the other hand, a solvent of high polarity stabilizes the $\text{CO}_2^{\cdot-}$ anion radicals in the liquid phase, enabling them to form formate ions upon reaction with protons.

4.4.3 Surface Derivatization for Controlling the Distribution of Products

Derivatization of the photocatalyst can be applied not only to control the adsorption of reactants, but also to govern desorption of products. A good example is the reduction of CO_2 by CdS that had been derivatized with thiolated self-assembled monolayers (SAMs).⁸⁵ Figure 4.11, prepared for this chapter based on the reported results, presents the ratio between the two major products, CO and HCOOH, as a function of surface coverage by the SAMs. Evidently, increasing the coverage increased the HCOOH/CO ratio. The solvent here was acetonitrile; however, the same trend (but not same values) was found also with dichloromethane. The results were explained by the fact that the surface modifiers were attached to the Cd^{2+} sites, thus reducing the area available for adsorption of the intermediate species $\text{CO}_2^{\cdot-}$ anion radicals. Consequently, the rate of CO formation was reduced.

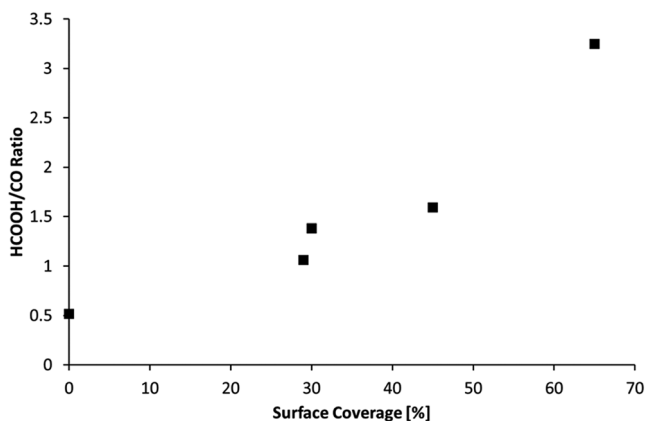


Figure 4.11 Ratio between the end-products HCOOH and CO in the photocatalytic reduction of CO_2 by CdS that had been partially derivatized by thiolated self-assembled monolayers. The data for this figure was taken from ref. 85.

4.5 Summary and Perspectives

The need to develop means to obtain specificity becomes more and more clear. On the reactants side, this is inevitable, as research evolves from laboratory scale studies to the handling of real streams that contain mixtures of contaminants. The evolution in the field towards integrating AOP (advanced oxidation processes) with active sludge biological treatment adds to this need. In parallel, on the products' side, there is a growing demand to go beyond simple degradation to the production of products having economic value. Although the subject of specificity was never at the center of attention in the photocatalysis research, an increase in awareness of specificity can be expected. Despite the relatively scarce data on specific photodegradation, it is still possible to define and discuss several approaches by which specificity can be obtained.

Generally speaking, the ways by which specificity may be obtained can be divided into approaches that operate by controlling adsorption, approaches that operate by controlling the reaction mechanism and approaches that act through controlling the desorption of products. In general, selective adsorption is the main vehicle for preferential degradation, whereas the other two approaches may be responsible for product selectivity. Among the various ways to achieve preferential degradation, molecular imprinting seems to be the most promising, as it combines high stability with superb specificity. However, there is a lot of room for developing and improvement. In particular, there is a need to study the following subjects: (a) correlation between size, geometry and performance; (b) stability of imprinted cavities; (c) blocking of activity in-between the imprinted sites; (d) prospects and limitations of using pseudo-target molecules; and (e) imprinting in non-TiO₂ photocatalysts.

With respect to product selectivity the major problem of controlling partial oxidation is largely unsolved. Although there are numerous cases where partial oxidation was reported, the situation is far from being satisfactory in terms of yield, selectivity and diversity. All these problems are still awaiting the right researchers.

References

1. H. Gerischer and A. Heller, *J. Phys. Chem.*, 1991, **95**, 5261.
2. D. Mantzavinos and E. Psillakis, *J. Chem. Technol. Biotechnol.*, 2004, **79**, 431.
3. J. P. Scott and D. F. Ollis, *Environ. Prog.*, 1995, **14**, 88.
4. J. Peller, O. Wiest and P. V. Kamat, *Environ. Sci. Technol.*, 2003, **37**, 1926.
5. M. R. Nimlos, W. A. Jacoby, D. M. Blake and T. A. Milne, *Environ. Sci. Technol.*, 1993, **27**, 732.
6. Y. Paz, *C. R. Chim.*, 2006, **9**, 774.
7. Y. Li, G. Lu and S. Li, *Chemosphere*, 2003, **52**, 843.
8. K. Wang, Y. Hsieh, M. Chou and C. Chang, *Appl. Catal., B*, 1999, **21**, 1.

9. C. S. Turchi and D. F. Ollis, *J. Catal.*, 1990, **122**, 178.
10. H. Haick and Y. Paz, *J. Phys. Chem. B*, 2001, **105**, 3045.
11. E. Zemel, H. Haick and Y. Paz, *J. Adv. Oxid. Technol.*, 2002, **5**, 27.
12. T. Tatsuma, S. Tachibana, T. Miwa, D. A. Tryk and A. Fujishima, *J. Phys. Chem. B*, 1999, **103**, 8033.
13. O. Zahraa, L. Sauvanaud, G. Hamard and M. Bouchy, *Int. J. Photoenergy*, 2003, **5**, 87.
14. X. Wang, S. Pehkonen and A. K. Ray, *Electrochim. Acta*, 2004, **49**, 1435.
15. M. Abdullah, G. K. Low and R. W. Matthews, *J. Phys. Chem.*, 1990, **94**, 6820.
16. C. B. Almquist and P. Biswas, *Appl. Catal., A*, 2001, **214**, 259.
17. B. Liu, T. Torimoto and H. Yoneyama, *J. Photochem. Photobiol., A*, 1998, **115**, 227.
18. K. Wang, Y. Hsieh and L. Chen, *J. Hazard. Mater.*, 1998, **59**, 251.
19. A. Fernandez-Nieves and F. De Las Nieves, *Colloids Surf., A*, 1999, **148**, 231.
20. D. H. Kim and M. A. Anderson, *J. Photochem. Photobiol., A*, 1996, **94**, 221.
21. J. E. Duffy, M. A. Anderson, C. G. Hill and W. A. Zeltner, *Ind. Eng. Chem. Res.*, 2000, **39**, 3698.
22. D. Robert, A. Piscopo and J. V. Weber, *Sol. Energy*, 2004, **77**, 553.
23. J. Theurich, M. Lindner and D. Bahnemann, *Langmuir*, 1996, **12**, 6368.
24. M. C. Blount, D. H. Kim and J. L. Falconer, *Environ. Sci. Technol.*, 2001, **35**, 2988.
25. D. S. Muggli and L. Ding, *Appl. Catal., B*, 2001, **32**, 181.
26. L. R. Matthews, D. Avnir, A. D. Modestov, S. Sampath and O. Lev, *J. Sol-Gel Sci. Technol.*, 1997, **8**, 619.
27. H. Hidaka, K. Nohara, J. Zhao, N. Serpone and E. Pelizzetti, *J. Photochem. Photobiol., A*, 1992, **64**, 247.
28. K. Inumaru, M. Murashima, T. Kasahara and S. Yamanaka, *Appl. Catal., B*, 2004, **52**, 275.
29. O. V. Makarova, T. Rajh, M. C. Thurnauer, A. Martin, P. A. Kemme and D. Cropek, *Environ. Sci. Technol.*, 2000, **34**, 4797.
30. T. Tsumura, N. Kojitani, I. Izumi, N. Iwashita, M. Toyoda and M. Inagaki, *J. Mater. Chem.*, 2002, **12**, 1391.
31. J. Matos, J. Laine and J. Herrmann, *Appl. Catal., B*, 1998, **18**, 281.
32. J. Matos, J. Laine and J. Herrmann, *J. Catal.*, 2001, **200**, 10.
33. T. Torimoto, S. Ito, S. Kuwabata and H. Yoneyama, *Environ. Sci. Technol.*, 1996, **30**, 1275.
34. N. Takeda, T. Torimoto, S. Sampath, S. Kuwabata and H. Yoneyama, *J. Phys. Chem.*, 1995, **99**, 9986.
35. S. Sampath, H. Uchida and H. Yoneyama, *J. Catal.*, 1994, **149**, 189.
36. N. Takeda, M. Ohtani, T. Torimoto, S. Kuwabata and H. Yoneyama, *J. Phys. Chem. B*, 1997, **101**, 2644.
37. A. Avraham-Shinman and Y. Paz, *Isr. J. Chem.*, 2006, **46**, 33.
38. G. Dagan, S. Sampath and O. Lev, *Chem. Mater.*, 1995, **7**, 446.
39. H. Haick and Y. Paz, *ChemPhysChem*, 2003, **4**, 617.

40. M. C. Lee and W. Choi, *J. Phys. Chem. B*, 2002, **106**, 11818.
41. S. Ghosh-Mukerji, H. Haick, M. Schwartzman and Y. Paz, *J. Am. Chem. Soc.*, 2001, **123**, 10776.
42. S. Ghosh-Mukerji, H. Haick and Y. Paz, *J. Photochem. Photobiol., A*, 2003, **160**, 77.
43. K. A. Connors, *Chem. Rev.*, 1997, **97**, 1325.
44. J. Lee and S. Park, *J. Phys. Chem. B*, 1998, **102**, 9940.
45. E. E. Tucker and S. D. Christian, *J. Am. Chem. Soc.*, 1984, **106**, 1942.
46. Y. Sagatelian, D. Sharabi and Y. Paz, *J. Photochem. Photobiol., A*, 2005, **174**, 253.
47. K. Ranjit, I. Willner, S. Bossmann and A. Braun, *Environ. Sci. Technol.*, 2001, **35**, 1544.
48. H. Tada, K. Teranishi, Y. Inubushi and S. Ito, *Langmuir*, 2000, **16**, 3304.
49. M. Nussbaum, N. Shaham-Waldmann and Y. Paz, *J. Photochem. Photobiol., A*, 2014, **290**, 11.
50. S. Y. Park, S. H. Kim, M. H. Lee, K. No, J. H. Lee and J. S. Kim, *Bull. Korean Chem. Soc.*, 2011, **32**, 741.
51. H. Yoneyama, S. Haga and S. Yamanaka, *J. Phys. Chem.*, 1989, **93**, 4833.
52. F. X. Llabrés i Xamena, P. Calza, C. Lamberti, C. Prestipino, A. Damin, S. Bordiga, E. Pelizzetti and A. Zecchina, *J. Am. Chem. Soc.*, 2003, **125**, 2264.
53. B. J. Aronson, C. F. Blanford and A. Stein, *Chem. Mater.*, 1997, **9**, 2842.
54. F. Dickey, *Proc. Natl. Acad. Sci. U. S. A.*, 1949, **35**, 227.
55. G. Shustak, S. Marx, I. Turyan and D. Mandler, *Electroanalysis*, 2003, **15**, 398.
56. S. Lee, I. Ichinose and T. Kunitake, *Langmuir*, 1998, **14**, 2857.
57. M. Lahav, A. B. Kharitonov, O. Katz, T. Kunitake and I. Willner, *Anal. Chem.*, 2001, **73**, 720.
58. M. Nussbaum and Y. Paz, *Handbook of Molecular Imprinting Advanced Sensor Applications*, ed. S. W. Lee and T. Kunitake, Pan Stanford Publishing House Ltd., Singapore, 2012, ch. 8, pp. 255–325.
59. S. Yamabi and H. Imai, *Thin Solid Films*, 2003, **434**, 86.
60. X. Shen, L. Zhu, G. Liu, H. Tang, S. Liu and W. Li, *New J. Chem.*, 2009, **33**, 2278.
61. X. Shen, L. Zhu, C. Huang, H. Tang, Z. Yu and F. Deng, *J. Mater. Chem.*, 2009, **19**, 4843.
62. X. Shen, L. Zhu, H. Yu, H. Tang, S. Liu and W. Li, *New J. Chem.*, 2009, **33**, 1673.
63. Y. Liu, R. Liu, C. Liu, S. Luo, L. Yang, F. Sui, Y. Teng, R. Yang and Q. Cai, *J. Hazard. Mater.*, 2010, **182**, 912.
64. D. Sharabi and Y. Paz, *Appl. Catal., B*, 2010, **95**, 169.
65. X. Shen, L. Zhu, J. Li and H. Tang, *Chem. Commun.*, 2007, 1163.
66. X. Shen, L. Zhu, G. Liu, H. Yu and H. Tang, *Environ. Sci. Technol.*, 2008, **42**, 1687.
67. J. Chen, D. F. Ollis, W. H. Rulkens and H. Bruning, *Water Res.*, 1999, **33**, 661.

68. M. Muneer, H. K. Singh and D. Bahnemann, *Chemosphere*, 2002, **49**, 193.
69. S. T. Martin, H. Herrmann, W. Choi and M. R. Hoffmann, *J. Chem. Soc., Faraday Trans.*, 1994, **90**, 3315.
70. C. M. Wang, A. Heller and H. Gerischer, *J. Am. Chem. Soc.*, 1992, **114**, 5230.
71. W. Choi, A. Termin and M. R. Hoffmann, *Angew. Chem., Int. Ed. Engl.*, 1994, **33**, 1091.
72. M. Lindner, J. Theurich and D. W. Bahnemann, *Water Sci. Technol.*, 1997, **35**, 79.
73. N. Z. Muradov, T. Ali, D. Muzzey, C. R. Painter and M. R. Kemme, *Sol. Energy*, 1996, **56**, 445.
74. N. N. Lichtin, M. Avudaithai, E. Berman and J. Dong, *Res. Chem. Intermed.*, 1994, **20**, 755.
75. Y. Luo and D. F. Ollis, *J. Catal.*, 1996, **163**, 1.
76. N. Lichtin, M. Avudaithai, E. Berman and A. Grayfer, *Sol. Energy*, 1996, **56**, 377.
77. F. Chen, J. Zhao and H. Hidaka, *Int. J. Photoenergy*, 2003, **5**, 209.
78. A. Molinari, R. Amadelli, L. Antolini, A. Maldotti, P. Battioni and D. Mansuy, *J. Mol. Catal. A: Chem.*, 2000, **158**, 521.
79. A. G. Agrios, K. A. Gray and E. Weitz, *Langmuir*, 2004, **20**, 5911.
80. X. Yan, T. Ohno, K. Nishijima, R. Abe and B. Ohtani, *Chem. Phys. Lett.*, 2006, **429**, 606.
81. M. Rochkind, S. Pasternak and Y. Paz, *Molecules*, 2014, **20**, 88.
82. K. Shimizu, T. Kaneko, T. Fujishima, T. Kodama, H. Yoshida and Y. Kitayama, *Appl. Catal., A*, 2002, **225**, 185.
83. V. Grimberg, M. Sc. thesis, Technion, Israel, 2002.
84. P. Boarini, V. Carassiti, A. Maldotti and R. Amadelli, *Langmuir*, 1998, **14**, 2080.
85. B. Liu, T. Torimoto and H. Yoneyama, *J. Photochem. Photobiol., A*, 1998, **113**, 93.